R. & M. No. 3010
(17,751)
A.R.C. Technical Report

MINISTRY OF SUPPLY

AERONAUTICAL RESEARCH COUNCIL
REPORTS AND MEMORANDA

Derivative Measurements and Flutter Tests on a Rectangular Wing with a Full-Span Control Surface, Oscillating in Modes of Wing Roll and Aileron Rotation

By

W. G. MOLYNEUX, B.Sc. and F. RUDDLESDEN, A.M.I.E.I.

LONDON: HER MAJESTY'S STATIONERY OFFICE

1957

EIGHT SHILLINGS NET

Derivative Measurements and Flutter Tests on a Rectangular Wing with a Full-Span Control Surface, Oscillating in Modes of Wing Roll and Aileron Rotation

By

W. G. Molyneux, B.Sc. and F. Ruddlesden, A.M.I.E.I.

Communicated by the Principal Director of Scientific Research (Air), Ministry of Supply

Reports and Memoranda No. 3010*

February, 1955

Summary.—Details are given of tests to measure the aerodynamic coefficients for a rectangular wing with a full-span aileron oscillating in modes of wing roll and aileron rotation. A new technique was used in which aileron rotation was geared to wing roll so that oscillation occurred in both degrees of freedom simultaneously.

The measured coefficients are compared with those derived from two-dimensional theory, and with coefficients estimated by an empirical method. The agreement with theory is poor but the estimated coefficients agree well with those measured.

Flutter calculations for the system were made, using both measured and theoretical derivatives, and the results are compared with flutter test results. The calculated flutter speed using measured derivatives agrees closely with that measured, whereas using theoretical derivatives the agreement is poor.

1. *Introduction.*—In flutter calculations the greatest uncertainty lies in the values of the aerodynamic coefficients to be used. In general, coefficients based on flat-plate theory[1, 2] are used, but there is some evidence that theoretical values of the coefficients may differ considerably from measured values, particularly in the case of control-surface coefficients[3]. There is an obvious need for more measurements of the aerodynamic coefficients for oscillating aerofoils, if only those for rigid aerofoils oscillating in simple modes, so as to provide information to compare with theory.

In the present report results are given of measurements of the aerodynamic coefficients for a rigid wing of finite aspect ratio with a full-span aileron, oscillating in modes of wing roll and aileron rotation. Wing-rolling–moment coefficients and aileron-hinge–moment coefficients were measured. A new technique was used for the measurements in which the aileron rotation was mechanically geared to the wing-rolling motion so that oscillations occurred in both degrees of freedom simultaneously. The large oscillatory forces resulting from the inertias of the wing and aileron were eliminated by counterbalancing them by springs at the excitation frequency, thus enabling a sensitive measurement of the residual aerodynamic forces to be made.

Equivalent constant-strip derivatives are derived from the measured aerodynamic coefficients, and are compared with values obtained from two-dimensional theory and with estimated values based on steady-flow measurements. Flutter calculations for the system were made using both measured and theoretical derivatives and the results are compared with the results of actual flutter tests.

* R.A.E. Report Structures 172, received 14th July, 1955.

2. *Description of the Method.*—The basis of the method is to gear together the aileron-rotation and wing-rolling motions using a mechanical linkage, the phase angle between the motions being either 0 deg or 180 deg. The separate motions of aileron rotation and wing roll are spring constrained, and the still-air resonance frequencies of each separate motion are adjusted to be equal and the same as the frequency of excitation of the system. Measurements are made of the forces at the gearing and excitation points, and by a suitable mass-balance arrangement these forces can be reduced to the small residual forces due to structural damping. The system is then excited in an air-stream with the frequency of excitation unchanged and the forces again measured, and by repeating these measurements with different gear ratios the required aerodynamic coefficients can be obtained.

It may be noted that the modes of oscillation for a wing-aileron system geared in this way are different from those used in current methods of measurement. By current methods the tests are done in two stages; firstly with the aileron locked to the wing and the wing excited, and secondly with the wing held stationary and the aileron excited. With the geared system wing and aileron moved simultaneously, and for the present system there is a straight nodal line for the aileron that passes through the intersection of the aileron-hinge line with the roll axis. There is also a variation in the amplitude ratio between wing and aileron motions with variation of gear ratio (a feature that is not present in current methods of measurement). However, for all systems of measurement it is assumed that the aerodynamic forces for the separate degrees of freedom of an oscillating structure can be superimposed to obtain the forces in a mode which combines these freedoms; and the aerodynamic coefficients obtained using the geared technique should, therefore, correspond with those obtained using other methods. On the other hand the technique enables a considerable reduction in the time required by current methods to balance out the still-air inertia forces of the oscillatory system.

2.1. *Equations of Motion for the System.*—The system is shown diagrammatically in Fig. 1. The aileron gear lever is held fixed at B by the force F_2 and the system is excited sinusoidally by the force F_1 at A. As the wing rolls through an angle ϕ the aileron rotates through an angle β, where the gear ratio $N = \beta/\phi$, and N is considered positive for motion in the sense shown in Fig. 1. Roll of the wing and rotation of the aileron are resisted by springs K_1 and K_2.

By resolving forces and taking moments it can be shown that the equations of motion for the still-air condition are:

$$\left.\begin{aligned} F_1 l_1 - F_2 l_2 &= K_1\phi + D_1\dot{\phi} + I_1\ddot{\phi} + I_{12}\ddot{\beta} \\ F_2 l_3 &= I_{12}\ddot{\phi} + K_2\beta + D_2\dot{\beta} + I_2\ddot{\beta} \end{aligned}\right\} \quad \ldots \quad (1)$$

Now if the system is dynamically balanced so that the product of inertia I_{12} about the roll and pitch axes is zero, and if the springs K_1 and K_2 are adjusted so that the natural frequencies of wing and aileron in roll, and aileron only in rotation about the hinge line are equal, and are the same as the frequency of the exciting force F_1, then:

$$\left.\begin{aligned} I_{12} &= 0 \\ -K_1\phi &= I_1\ddot{\phi} \\ -K_2\beta &= I_2\ddot{\beta} \end{aligned}\right\} \quad \ldots \quad (2)$$

Equations (1) then reduce to:

$$\left.\begin{aligned} F_1 l_1 - F_2 l_2 &= D_1\dot{\phi} \\ F_2 l_3 &= D_2\dot{\beta} \end{aligned}\right\} \quad \ldots \quad (3a)$$

and since $\dot{\beta}/\dot{\phi} = N$, $l_2/l_3 = N$ equations (3a) may be written:

$$\left.\begin{aligned} F_1 l_1 - F_2 l_2 &= D_1\dot{\phi} \\ F_2 l_2 &= N^2 D_2\dot{\phi} \end{aligned}\right\} \quad \ldots \quad (3b)$$

The still-air forces F_1 and F_2 are therefore reduced to the (small) forces due to damping only, and vary with magnitude but are independent of the sign of the gear ratio. The inertia and stiffness forces balance for all gear ratios.

Now consider the system to be oscillated in an air stream with the excitation frequency unchanged. The aerodynamic rolling moment and aileron-hinge moment are:

$$\left.\begin{aligned}\frac{\text{Rolling moment}}{\rho V^2 S c_m} &= (\bar{L}_\phi \phi + \bar{L}_\beta \beta)\\ \frac{\text{Hinge moment}}{\rho V^2 S c_m} &= (\bar{H}_\phi \phi + \bar{H}_\beta \beta)\end{aligned}\right\}, \quad \ldots \quad (4)$$

and these aerodynamic forces are reacted by additional forces $\bar{F}_1'$ and $\bar{F}_2'$ at A and B, where:

$$\left.\begin{aligned}\bar{F}_1' l_1 - \bar{F}_2' l_2 &= \rho V^2 S c_m (\bar{L}_\phi \phi + \bar{L}_\beta \beta)\\ \bar{F}_2' l_3 &= -\rho V^2 S c_m (\bar{H}_\phi \phi + \bar{H}_\beta \beta)\end{aligned}\right\}. \quad \ldots \quad (5a)$$

Substituting for β and l_3 we have:

$$\left.\begin{aligned}\bar{F}_1' l_1 - \bar{F}_2' l_2 &= \rho V^2 S c_m \phi (\bar{L}_\phi + N \bar{L}_\beta)\\ \bar{F}_2' l_2 &= -V^2 S c_m \phi N (\bar{H}_\phi + N \bar{H}_\beta)\end{aligned}\right\}. \quad \ldots \quad (5b)$$

$\bar{L}_\phi$, $\bar{L}_\beta$, $\bar{H}_\phi$ and $\bar{H}_\beta$ are the complex aerodynamic force coefficients and may be written:

$$\left.\begin{aligned}\bar{L}_\phi &= (L_\phi + i\nu L_{\dot{\phi}})\\ \bar{L}_\beta &= (L_\beta + i\nu L_{\dot{\beta}})\end{aligned}\right\}, \quad \ldots \quad (6)$$

etc.,

i.e., in the form of an aerodynamic stiffness coefficient for the force in phase with the motion, and an aerodynamic damping coefficient for the force in quadrature with the motion.

Similarly the complex forces $\bar{F}_1'$ and $\bar{F}_2'$ may be written:

$$\left.\begin{aligned}\bar{F}_1' &= (F_1' + i\dot{F}_1')\\ \bar{F}_2' &= (F_2' + i\dot{F}_2')\end{aligned}\right\}. \quad \ldots \quad (7)$$

Substituting equations (6) and (7) in equations (5*b*), and equating real and imaginary parts, we have:

(1) aerodynamic forces in phase with roll motion

$$\left.\begin{aligned}F_1' l_1 - F_2' l_2 &= \rho V^2 S c_m \phi (L_\phi + N L_\beta)\\ F_2' l_2 &= -\rho V^2 S c_m \phi N (H_\phi + N H_\beta)\end{aligned}\right\}. \quad \ldots \quad (8a)$$

(2) aerodynamic forces in quadrature with roll motion

$$\left.\begin{aligned}\dot{F}_1' l_1 - \dot{F}_2' l_2 &= \rho V^2 S c_m \phi \nu (L_{\dot{\phi}} + N L_{\dot{\beta}})\\ \dot{F}_2' l_2 &= -\rho V^2 S c_m \phi \nu N (H_{\dot{\phi}} + N H_{\dot{\beta}})\end{aligned}\right\}. \quad \ldots \quad (8b)$$

Further, the frequency parameter ν is given by $\nu = \omega c_m / V$, where ω is the frequency of excitation of the system. Therefore, equations (8*b*) may be written:

$$\left.\begin{aligned}\dot{F}_1' l_1 - \dot{F}_2' l_2 &= \rho V S c_m^2 \omega \phi (L_{\dot{\phi}} + N L_{\dot{\beta}})\\ \dot{F}_2' l_2 &= -\rho V S c_m^2 \omega \phi N (H_{\dot{\phi}} + N H_{\dot{\beta}})\end{aligned}\right\}. \quad \ldots \quad (8c)$$

By measuring the ' in phase ' and quadrature components of $\bar{F}_1'$ and $\bar{F}_2'$ for a range of gear ratios, and plotting them against the gear ratio, N, graphs can be constructed from which the values of the aerodynamic coefficients for wing-rolling moment and aileron-hinge moment can be obtained.

3. *Details of the Rig.*—The rig, with reflector plate removed, can be seen in Fig. 2a and the main dimensions are given in Table 1. It consisted of a vertically mounted half-wing, free to roll about the root end, with a full-span round-nosed aileron, the ratio aileron chord/wing chord being 0·20. The wing aspect ratio was 4·05 and the aerofoil section was RAE 101. Bearings for the aileron were at the root and tip, and a further bearing for the aileron torque tube was provided below the roll axis (Fig. 2b). Bending flexibility of the aileron was kept to a minimum by bracing it by a king post at mid-span.

The wing main spar extended below the roll axis, and helical springs from this member to the mounting frame provided stiffness in roll. A torsion bar of adjustable length between the aileron torque tube and the main spar provided stiffness in aileron rotation.

3.1. *Gearing and Mass-balance Arrangement.*—The arrangement for gearing wing roll to aileron rotation, and the mass-balance arrangement for adjusting product of inertia of the system are shown in Fig. 2b. A gear lever was rigidly attached to the aileron torque tube and points on the gear lever could be coupled to a force-measuring gauge on the mounting frame through a ball-ended gear rod. By coupling different points on the gear lever to the force gauge different gear ratios were obtained. The gear lever also carried a grooved disc concentric with the aileron torque tube and to this disc were attached two mass-balance weights. These weights could be slid around the groove in the disc to vary the product of inertia of the wing–aileron system without affecting the moment of inertia of the aileron itself.

3.2. *Excitation System.*—The method of excitation is shown diagrammatically in Fig. 3. The wing was excited at about mid-span through a rod driven sinusoidally by a rider on a rotating swash plate. The tilt of the swash plate could be varied whilst rotating to vary the throw of the rider from zero to about plus or minus one inch. The coupling between exciter rod and rider was through a force gauge and spring, the force gauge measuring the force in the rod and the spring serving as a filter to reduce the amplitude of harmonics of the basic excitation frequency. It should be noted that the exciter coupling spring is not part of the system considered in section 2.1, and the presence of this spring introduced some difficulties during the wind-tunnel tests (*see* section 6).

3.3. *Force and Amplitude Gauges.*—The gauges used for force measurements at the gearing and excitation points were as shown in Fig. 4. The gauge comprised two thin steel strips attached to a rigid frame and pretensioned by a draw bolt at the centre to form an X, with an angle of about 20 deg between the strips. Strain-gauges of about 2,400 ohms resistance were cemented to the strips and were connected as a Wheatstone bridge (with 36 volts applied) to respond to a force in the applied force direction. The strips were pretensioned for a load of about plus or minus 30 lb, and the gauge output was linear with applied load for loads up to this value. The output ceased to be linear when excessive loads caused one strip to slacken. Readings of gauge output were taken on a 1,300 ohm galvanometer with a scale sensitivity of 180 mm/microamp; and loads as low as 0·04 lb could be detected.

The amplitude gauge was a simple cantilever strip between the wing and mounting frame, with strain-gauges at the root end connected in a bridge circuit. The gauge output was measured with the galvanometer described above.

4. *Frequency Measurement.*—It is apparent from section 2.1 that the inertia and stiffness forces for the oscillating system are balanced at one particular frequency, and once this frequency has been established it must be maintained to a high order of accuracy throughout the tests. For the present tests the method used was to obtain an accurate measurement of frequency at intervals during the tests so that any deviations from the basic frequency could be detected and correction made.

The principle was to count the number of cycles output from a 600 c.p.s. crystal oscillator during 20 complete cycles of oscillations of the structure. The number of cycles from the crystal oscillator was displayed on a bank of electronic counting tubes, and by this method a measurement of frequency was obtained to an accuracy of about 0·1 per cent. An automatic repeat reading was displayed on the counter at ten-second intervals throughout the test, so that changes of frequency could be detected and manual adjustment made. In practice it was found possible to maintain the frequency constant to within about plus or minus 0·2 per cent.

5. *Force and Amplitude Measurement.*—The data for substitution in equations (8*a*) and (8*c*) of section 2.1 are required in the form of components of the aerodynamic forces in phase and in quadrature with the motion of the system. This information can be derived from measurements relative to some common datum, of amplitudes and phase angles of the vectors representing displacement of the system and the aerodynamic forces, or by measuring two components at 90 deg of these vectors relative to a common datum. For the present tests the latter approach was used.

The method was based on rectification at excitation frequency of the strain-gauge outputs from the amplitude and force gauges, using the circuits shown in Figs. 5a and 5c. A two-segment commutator, one half at positive potential and the other negative, was fitted to the shaft of the exciter motor, and from two pairs of brushes at 90 deg to each other two square-wave output signals at 90-deg phase angle were obtained. Each output could be selected and fed to the energising coil of a relay switch unit which carried the strain-gauge signal, thus reversing the signal for each half cycle of the commutator. The effect is seen in Fig. 6. Suppose the strain-gauge signal is of amplitude S_0 and that switching occurs at phase angles ψ, $\psi + 180$ deg, $\psi + 360$ deg, etc., from one pair of brushes, and at $\psi + 90$ deg, $\psi + 270$ deg, etc., from the other pair. Then the mean levels of the recitified signals due to switching are:

$$\left.\begin{aligned} \text{first pair} &= -\int_{\psi}^{\psi+180} \frac{S_0}{\pi} \sin\theta \, d\theta = -\frac{2S_0}{\pi}\cos\psi \\ \text{second pair} &= -\int_{\psi+90}^{\psi+270} \frac{S_0}{\pi} \sin\theta \, d\theta = \frac{2S_0}{\pi}\sin\psi \end{aligned}\right\} \quad \ldots \quad \ldots \quad (9)$$

$S_0 \cos\psi$ and $S_0 \sin\psi$ are components at 90 deg of S_0, with a factor $2/\pi$ due to rectification, and these mean levels can be measured on a sensitive, direct-current, damped galvanometer.

For the flutter test, where components of the amplitudes of the wing and aileron motions were required, there was no rotating component and the commutator method could not be used. For this test the circuit shown in Fig. 5b replaced that shown in Fig. 5a. It consisted of two pairs of contacts driven by the oscillating structure through a spring and a friction coupling respectively, to produce the required square-wave outputs at 90-deg phase angle for the relay switch unit. The latter method could have been used for both derivative and flutter tests, but in practice the contact setting was rather critical and the commutator system was preferred for the rather lengthy derivative measurements.

6. *Test Procedure.*—6.1. *Setting Up.*—The procedure in setting up the wing–aileron system was first to lock the wing rigidly to the mounting frame, disconnect the gear rod from the aileron lever, and adjust the aileron torsion bar to obtain a convenient frequency for the aileron. The frequency was measured by timing twenty cycles of decaying oscillation with the frequency counter. A frequency of 5·47 c.p.s. was chosen, being a stable speed for the exciter motor. The aileron was then rigidly locked to the wing, the wing lock was removed, and the wing was excited at the frequency obtained for the aileron. The roll springs were adjusted until the output from the excitation force gauge was a minimum, corresponding to a coincidence of the wing-roll frequency with the exciting frequency. The aileron lock was next removed, the gear rod recoupled to the lever, and the now geared system excited at the same frequency as before. The inertia balance weights on the aileron lever were slid around the grooved disc until a minimum output from the gear force gauge was obtained, and at this stage the setting-up operation was complete (*i.e.*, equations (2), section 2.1, were satisfied).

6.2. *Aerodynamic Force Measurements.*—The tests were made in the Royal Aircraft Establishment 5-ft Low-Speed Wind Tunnel. The model was vertically mounted in the tunnel with a reflector plate at the wing-root end to simulate the symmetric flow condition, so that roll of the wing was equivalent to a mode of symmetric linear bending. The tests were made within the speed range from 40 ft/sec to 240 ft/sec, corresponding to a range of frequency parameter from 1·29 to 0·21, and measurements of hinge moments and rolling moments were made for both steady and oscillatory conditions.

6.2.1. *Oscillatory force measurements.*—Initial measurements of force-gauge output with a fixed gear ratio and variation of roll amplitude showed that the aerodynamic forces tended to be non-linear with amplitude in the range considered. The non-linearity was eliminated by fitting a transition wire 1 mm. in diameter to both wing surfaces at 0·30-chord aft of the wing leading edge. The force measurements for each value of gear ratio (positive and negative) were made with the roll amplitude constant. However, as the gear ratio increased it was necessary to reduce roll angle to avoid excessive aileron angles. In no case did the aileron angle exceed plus or minus 8 deg and it was never less than plus or minus 3 deg. Force measurements were made at several wind speeds for each gear ratio, and the measurements were repeated at least once in each case to obtain an indication of the scatter of results. When the gear ratio was negative it was found that at certain wind speeds the system resonated, corresponding to a condition in which the aerodynamic stiffness was balanced by the stiffness of the exciter spring. In the region of this resonance it proved difficult to maintain a stable amplitude of oscillation for the wing, and the phase angle between wing and exciter motions became very sensitive to small changes of excitation frequency. In the force measurements, these effects were manifest by large fluctuations in the forces in quadrature with the motion. Resonance was approached at about 240 ft/sec with the gear ratio — 2·3, about 200 ft/sec with the gear ratio — 4·6 and about 140 ft/sec with the gear ratio — 9·2 (Figs. 8, 10 and 12).

6.2.2. *Steady force measurements.*—For these measurements the roll springs and aileron torsion bar were disconnected. With the gear ratio at 4·6 and a tunnel speed of 240 ft/sec the wing was then rolled to a fixed angle, thus rotating the aileron, and the outputs from the force gauges measured. From these measurements the wing-rolling moment due to aileron angle and aileron-hinge moment due to aileron angle were determined.

6.2.3. *Calibration of force gauges.*—The gauges were calibrated under both oscillatory and steady force conditions. For oscillatory calibrations, firstly a known weight was clamped to the exciter shaft and secondly a plate of known inertia was clamped to the aileron on the roll axis, and the increase in gauge outputs measured when the wing was oscillated through a range of amplitudes, with fixed gear ratio. The forces resulting from oscillation of the added weights were then calculated and the gauge factors found.

The gauge factors for steady flow were obtained by loading the gauges directly and measuring the gauge outputs.

The gauges were calibrated at the beginning and at the end of the tests and checks were made at intervals during the tests. Only slight changes of gauge calibration factors were obtained.

6.3. *Flutter Tests.*—For the flutter tests the gear rod was disconnected from the gear lever and the exciter rod disconnected from the wing. Thin cantilever strip amplitude gauges were then connected between the aileron gear lever and the wing main spar and between the wing and mounting frame. The square-wave generator (Fig. 5b) for the relay switch unit was coupled to the wing, and the aileron balance weights were slid around the disc so that the aileron was under-mass-balanced. The tunnel wind speed was then increased until flutter occurred, and at the flutter speed measurements were made of flutter speed, flutter frequency and the components of the outputs from the wing and aileron amplitude gauges. The results are given in Table 6.

6.3.1. *Calibrations.*—The gauges measuring aileron rotation relative to the wing and wing roll relative to the mounting frame were calibrated statically by rotating the wing and aileron through fixed angles and measuring the gauge outputs.

Measurements were also required of the stiffnesses and inertias of the wing–aileron system for use in subsequent flutter calculations. The stiffnesses in wing roll and aileron rotation were measured statically, by applying known torques to these components and measuring their angular rotations. Accurate measurements of the coupled and uncoupled frequencies of the wing–aileron system were then made, and from these frequencies and the measured stiffnesses the required direct- and cross-inertia values for the system were calculated. The values are given in Table 5.

7. *Derivation of the Aerodynamic Force Coefficients.*—The oscillatory aerodynamic forces at the excitation and gearing points, expressed as a function of wing-roll angle, are plotted for each gear ratio in Figs. 7 to 12. The forces in quadrature with the wing motion are plotted against tunnel windspeed, V, and those in phase with the motion are plotted against V^2. It may be noted that for gear ratio 9·2, wind speed 200 ft/sec (Fig. 11), no values for excitation force are plotted. At this speed the force was in fact in excess of the pretension limit for the gauge. There is appreciable scatter of results, even for repeat tests under essentially similar conditions. The scatter is particularly marked where the force measured is small (*e.g.*, quadrature hinge-moment components for gear ratios plus or minus 2·3) and where the aerodynamic resonance condition is approached. However, within the limits of experiment the force components in quadrature with the motion may be said to vary linearly with wind speed, V, and those in phase with the motion vary linearly with V^2.

From the equations of the mean lines for the quadrature and ' in phase ' components for each gear ratio, expressions for wing-rolling moments and aileron-hinge moments per radian roll, as functions of wind speed, were derived. The values are given in Table 2, and are shown plotted against gear ratio in Figs. 13 and 14. It can be seen that the wing-rolling moment and aileron-hinge moment functions vary approximately linearly with gear ratio; and, furthermore, the functions for ' in phase ' rolling moment and ' in phase ' and ' in quadrature ' hinge moments can be represented by lines that pass through the origin. The significance of the latter characteristic is that rolling moment due to roll displacement, hinge moment due to roll displacement and hinge moment due to roll velocity (force coefficients L_ϕ, H_ϕ and $H_{\dot\phi}$ respectively in equations (8*a*) and (8*c*)) are too small to be detected by the present technique*. The equations of the lines representing rolling moments and hinge moments as functions of wind speed and gear ratio were obtained, and by comparing these equations with equations (8*a*) and (8*c*), values for the hinge-moment and rolling-moment coefficients were derived. The values obtained are given, together with the coefficients derived from the steady-flow measurements in Table 3.

8. *Equivalent Constant-Strip Derivatives.*—An equivalent constant-strip derivative is defined as one which is chosen to be constant over the span and which when integrated over the span in the appropriate mode of oscillation will give the correct aerodynamic force in that mode. Therefore:

$$\left.\begin{aligned} \rho V^2 S c_m \bar{L}_\phi &= \textstyle\int_{\text{wing}} \rho V^2 \bar{l}_z y^2\, dy \\ \rho V^2 S c_m \bar{L}_\beta &= \textstyle\int_{\text{wing}} \rho V^2 c_m \bar{l}_\beta y\, dy \\ \rho V^2 S c_m \bar{H}_\phi &= \textstyle\int_{\text{aileron}} \rho V^2 c_m \bar{h}_z y\, dy \\ \rho V^2 S c_m \bar{H}_\beta &= \textstyle\int_{\text{aileron}} \rho V^2 c_m{}^2 \bar{h}_\beta\, dy \end{aligned}\right\}, \quad \ldots \quad (10)$$

where $\bar{l}_z$, $\bar{l}_\beta$, $\bar{h}_z$, $\bar{h}_\beta$ are the complex equivalent constant-strip derivatives and are of similar form to the complex force coefficients, equations (6).

The equivalent constant-strip derivatives form a useful basis for comparison with theoretical derivatives for two-dimensional flow. Their values are given in Table 4 and are compared with theoretical values in Figs. 15 and 16. It can be seen that there are considerable discrepancies between the ' measured ' and theoretical results. The discrepancy is particularly marked for the derivative $l_{\dot\beta}$, where the measured value is positive whereas the theoretical value is negative over most of the range of frequency parameter investigated. However, large differences between

* It should be noted that in equations (8*a*) and (8*c*) the aileron-hinge moments are given by $F_2' l_2/N$ and $\dot{F}_2' l_2/N$.

measured derivatives for a finite wing and theoretical values for two-dimensional flow are to be anticipated, particularly since other investigators[3] have found that such large differences between theory and experiment are common for control-surface coefficients, even where the measurements are made in two-dimensional flow.

8.1. *Estimation of Equivalent Constant-Strip Derivatives from Steady-Flow Measurements.*—A method has been suggested by Minhinnick whereby a closer approximation to the true oscillatory derivatives can be obtained than is provided by two-dimensional theory alone. The method requires the measurement of certain steady-flow stiffness derivatives and is based on the assumption that the oscillatory derivatives for a finite wing (aspect ratio not greater than about 4) do not vary with frequency parameter By Minhinnick's method the approximations to the equivalent constant oscillatory derivatives are given by:

$$\left.\begin{aligned}
&\text{oscillatory } l_z = 0\\
&\text{oscillatory } h_z = 0\\
&\text{oscillatory } l_{\dot{z}} = \text{steady flow } l_\alpha\\
&\text{oscillatory } h_{\dot{z}} = \text{steady flow } h_\alpha\\
&\text{oscillatory } l_\beta = \text{steady flow } l_\beta\\
&\text{oscillatory } h_\beta = \text{steady flow } h_\beta\\
&\text{oscillatory } l_\beta = \text{steady flow } l_\beta \times \frac{\text{maximum two-dimensional theory value of } l_\beta}{\text{minimum two-dimensional theory value of } l_\beta}\\
&\text{oscillatory } h_\beta = \text{steady flow } h_\beta \times \frac{\text{maximum two-dimensional theory value of } h_\beta}{\text{minimum two-dimensional theory value of } h_\beta}
\end{aligned}\right\} \quad \ldots \quad (11)$$

The derivatives l_α and h_α in the above equations are the steady-flow equivalent constant-strip derivatives as derived from measurements of wing-rolling moment and aileron-hinge moment due to wing incidence. Measurements of these forces were not made during the tests so that estimates for the derivatives $l_{\dot{z}}$ and $h_{\dot{z}}$ could not be obtained. Estimates for the remaining derivatives using the above equations are given in Table 4 and are compared with the measured and two-dimensional theory values in Figs. 15 and 16. It can be seen that the agreement between measured and estimated values is good.

9. *Flutter Calculations.*—Calculations of flutter characteristics for the wing–aileron system were made, firstly using the measured aerodynamic derivatives and secondly using the derivatives from two-dimensional theory. The results are given together with the measured results in Table 6. The calculations using measured derivatives give values for flutter speed, frequency, and frequency parameter in close agreement with those measured; for amplitude ratio and phase angle the agreement is not as good but might still be described as fair. The calculations with two-dimensional derivatives, on the other hand, give fair agreement for frequency, amplitude ratio and phase angle, but poor agreement for flutter speed and frequency parameter From the practical view-point it is the accurate prediction of flutter speeds that is most important, and in this respect the measured derivatives are much better than the two-dimensional derivatives.

A possible explanation for the discrepancies between the measured results and those calculated using measured derivatives may lie in the fact that rig structural damping was not included in the calculations. .The inclusion of structural damping in flutter calculations has, in general, a negligible effect on flutter speeds and frequencies, but the same may not be true of amplitude ratios and phase angles.

10. *Conclusions.*—The gearing technique for derivative measurements has proved successful and the oscillatory aerodynamic coefficients for wing-rolling moment and aileron-hinge moment have been obtained for a particular system. The coefficients, expressed as equivalent constant-strip derivatives, are compared with derivatives obtained using two-dimensional–flow theory,

and also with those estimated using a method proposed by Minhinnick. The theoretical derivatives for two-dimensional flow differ considerably from those measured whereas the estimated derivatives are in reasonable agreement with the measured values.

Flutter calculations have been made for the system, using both the measured derivatives and derivatives from two-dimensional theory, and the results are compared with actual flutter-test results. The calculated flutter speed using two-dimensional derivatives differs considerably from that measured whereas the calculated flutter speed using measured derivatives is in very close agreement with the measured value.

11. *Acknowledgements.*—Acknowledgements are due to Messrs. F. Smith, P. R. Guyett and D. R. Gaukroger for assistance in the design and development of the excitation and recording systems used for these tests.

NOTATION

D_1	Structural damping coefficient for wing roll
D_2	Structural damping coefficient for aileron rotation
F_1, F_2	Forces at excitation and gearing points for oscillation in still air
$\bar{F}_1', \bar{F}_2'$	Complex aerodynamic forces at excitation and gearing points for oscillation in wind stream
K_1, K_2	Spring stiffnesses resisting wing and aileron motions
N	Gear ratio between aileron rotation and wing roll ($= \beta/\phi$)
I_1	Inertia of wing plus aileron about roll axis
I_2	Inertia of aileron about hinge line
I_{12}	Product of inertia of aileron about hinge line and roll axis
$\bar{L}_\phi$	Complex non-dimensional wing-roll coefficient due to wing roll
$\bar{L}_\beta$	Complex non-dimensional wing-roll coefficient due to aileron rotation
$\bar{H}_\phi$	Complex non-dimensional aileron-hinge–moment coefficient due to wing roll
$\bar{H}_\beta$	Complex non-dimensional aileron-hinge–moment coefficient due to aileron rotation
S	Wing area
V	Wind speed
c_m	Wing mean chord
l_1	Distance of excitation point from roll axis
l_2	Distance of gearing point from roll axis
l_3	Distance of gearing point from aileron hinge ($= l_2/N$)
ϕ	Angle of roll of the wing
β	Angle of rotation of aileron relative to wing
ρ	Air density
ω	Frequency of excitation
ν	Frequency parameter ($= \omega c_m/V$)

REFERENCES

No.	*Author*	*Title, etc.*
1	I. T. Minhinnick	Subsonic aerodynamic derivatives for wings and control surfaces (compressible and incompressible flow). R.A.E. Report Struct. 87. A.R.C. 14, 228. July, 1950.
2	W. P. Jones	Aerodynamic forces on wings in simple harmonic motion. R. & M. 2026. February, 1945.
3	K. C. Wright	Measurement of two-dimensional derivatives on a wing-aileron-tab system. R. & M. 2934. October, 1952.

TABLE 1

Main Dimensions of Wing–Aileron System

Wing length from roll axis to tip	= 3·04 ft
Aileron length from roll axis to tip	= 3·00 ft (wing-tip rib extends over aileron)
Wing chord (including aileron)	= 1·5 ft
Aileron chord aft of hinge line (round-nosed control surface) ..	= 0·3 ft
Gap between aileron nose and wing	= $\frac{1}{32}$ in.
Wing area	= 4·56 sq ft
Aspect ratio	= 4·05
Wing/aileron chord ratio	= 0·20
Thickness/chord ratio	= 0·10
Aerofoil section	= RAE 101
Distance of excitation point from roll axis, l_1	= 18·2 in.
Distance of gearing points from roll axis, l_2	= 9·2 in.

TABLE 2

Wing-Rolling Moment and Aileron-Hinge Moment as Functions of Wind Speed for Different Gear Ratios

Gear ratio $\frac{\text{aileron angle}}{\text{roll angle}}$ N	Components relative to roll displacement											
	Force at excitation point per radian roll		Force at gearing point per radian roll		Rolling moment due to excitation force per radian roll		Rolling moment due to gearing force per radian roll		Total rolling moment per radian roll		Aileron-hinge moment per radian roll	
	In quadrature (lb/radn)	In phase (lb/radn)	In quadrature (lb/radn)	In phase (lb/radn)	In quadrature (lb/radn)	In phase (lb ft/radn)	In quadrature (lb ft/radn)	In phase (lb ft/radn)	In quadrature (lb ft/radn)	In phase (lb ft/radn)	In quadrature (lb ft/radn)	In phase (lb ft/radn)
+2·3 ..	$-0\cdot880\times V$	$-1\cdot44\times10^{-2}V^2$	$-0\cdot026\times V$	$-0\cdot097\times10^{-2}V^2$	$-1\cdot33\times V$	$-2\cdot18\times10^{-2}V^2$	$+0\cdot020\times V$	$+0\cdot074\times V$	$-1\cdot31\times V$	$-2\cdot11\times10^{-2}V^2$	$-0\cdot0087\times V$	$-0\cdot0323\times10^{-2}V^2$
−2·3 ..	$-0\cdot738\times V$	$+1\cdot42\times10^{-2}V^2$	$-0\cdot025\times V$	$-0\cdot103\times10^{-2}V^2$	$-1\cdot12\times V$	$+2\cdot16\times10^{-2}V^2$	$0\cdot019\times V$	$0\cdot079\times V$	$-1\cdot10\times V$	$+2\cdot24\times10^{-2}V^2$	$+0\cdot0083\times V$	$+0\cdot0343\times10^{-2}V^2$
+4·6 ..	$-1\cdot015\times V$	$-3\cdot05\times10^{-2}V^2$	$-0\cdot114\times V$	$-0\cdot390\times10^{-2}V^2$	$-1\cdot54\times V$	$-4\cdot63\times10^{-2}V^2$	$0\cdot087\times V$	$0\cdot299\times V$	$-1\cdot45\times V$	$-4\cdot33\times10^{-2}V^2$	$-0\cdot0190\times V$	$-0\cdot0650\times10^{-2}V^2$
−4·6 ..	$-0\cdot760\times V$	$+2\cdot86\times10^{-2}V^2$	$-0\cdot105\times V$	$-0\cdot400\times10^{-2}V^2$	$-1\cdot15\times V$	$+4\cdot33\times10^{-2}V^2$	$0\cdot081\times V$	$0\cdot307\times V$	$-1\cdot07\times V$	$+4\cdot64\times10^{-2}V^2$	$+0\cdot0175\times V$	$+0\cdot0667\times10^{-2}V^2$
+9·2 ..	$-1\cdot270\times V$	$-6\cdot55\times10^{-2}V^2$	$-0\cdot413\times V$	$-1\cdot525\times10^{-2}V^2$	$-1\cdot92\times V$	$-9\cdot93\times10^{-2}V^2$	$0\cdot317\times V$	$1\cdot170\times V$	$-1\cdot60\times V$	$-8\cdot76\times10^{-2}V^2$	$-0\cdot0344\times V$	$-0\cdot127\times10^{-2}V^2$
−9·2 ..	$-0\cdot740\times V$	$+5\cdot06\times10^{-2}V^2$	$-0\cdot430\times V$	$-1\cdot500\times10^{-2}V^2$	$-1\cdot12\times V$	$+7\cdot67\times10^{-2}V^2$	$+0\cdot330\times V$	$+1\cdot150\times V$	$-0\cdot79\times V$	$+8\cdot82\times10^{-2}V^2$	$+0\cdot0358\times V$	$+0\cdot125\times10^{-2}V^2$

Note : Wind speed V is in ft/sec

TABLE 3

Measured Values for Rolling-Moment and Hinge-Moment Coefficients

Coefficient	Oscillatory flow value	Steady flow value
L_ϕ	0	0
$L_{\dot{\phi}}$	1·45	0
L_β	0·593	0·667
$L_{\dot{\beta}}$	0·0527	0
H_ϕ	0	0
$H_{\dot{\phi}}$	0	0
H_β	−0·0085	−0·00824
$H_{\dot{\beta}}$	−0·00458	0

TABLE 4

Comparison of Measured Equivalent Constant-Strip Derivatives with Estimated Values

Derivative	Measured value	Derived value
l_z	0	0
$l_{\dot{z}}$	1·06	—
h_z	0	0
$h_{\dot{z}}$	0	—
l_β	0·602	0·675
$l_{\dot{\beta}}$	0·0533	0·0810
h_β	−0·00861	−0·00833
$h_{\dot{\beta}}$	−0·00464	−0·00437

TABLE 5

Stiffness and Inertia Details of Wing–Aileron System

Roll inertia (wing + aileron) about roll axis	= 2·0 slugs ft²
Aileron inertia about hinge line	= 0·00645 slugs ft²
Aileron product of inertia about roll axis and aileron-hinge line	= 0·015 slugs ft²
Wing roll stiffness about roll axis	= 2030 lb ft/radn
Aileron rotation stiffness about hinge line	= 8·25 lb ft/radn

TABLE 6

Comparison of Measured and Calculated Flutter Values

	Measured in flutter test	Calculated using measured derivatives	Calculated using two-dimensional derivatives
Flutter speed (ft/sec)	64·5	63·2	43·9
Flutter frequency (c.p.s.) ..	5·42	5·61	5·63
Flutter frequency parameter ..	0·79	0·84	1·21
Phase angle roll leading aileron ..	29°	17° 30′	24° 18′
Amp. ratio $\frac{\text{Roll angle}}{\text{Aileron angle}}$	0·069	0·044	0·041

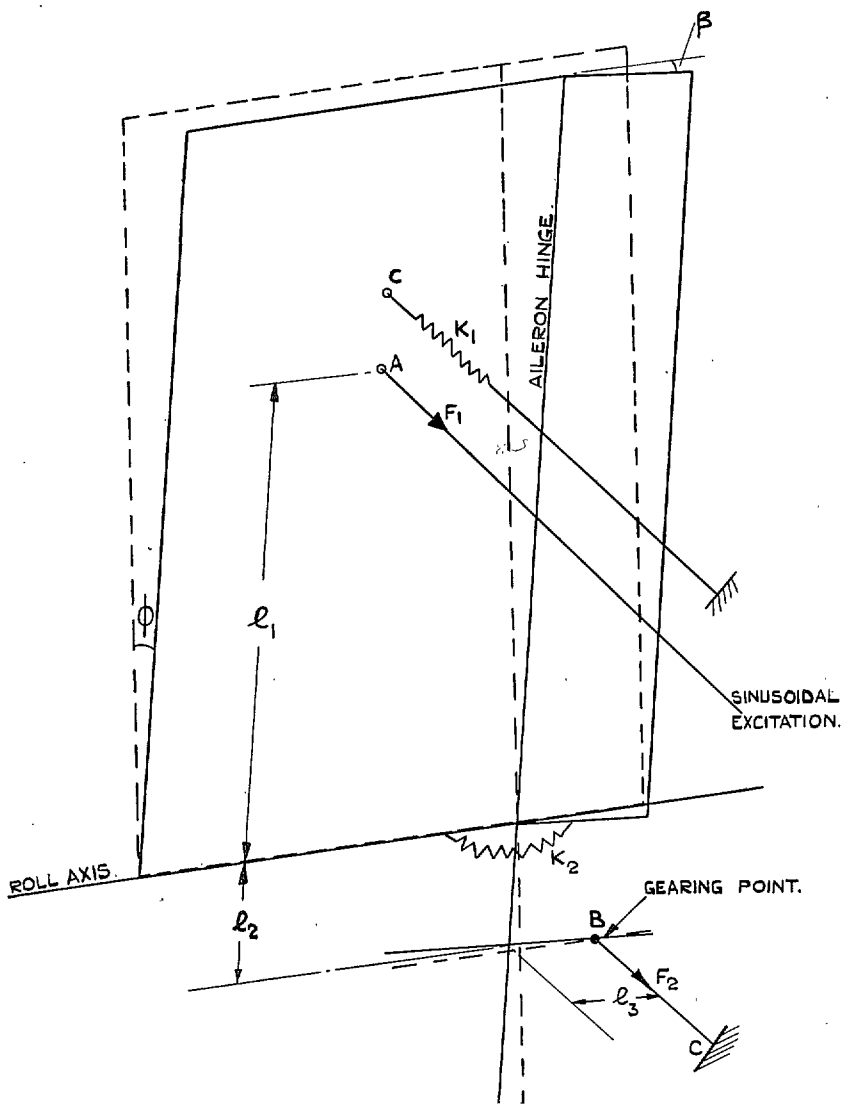

FIG. 1. Wing roll geared to aileron rotation.

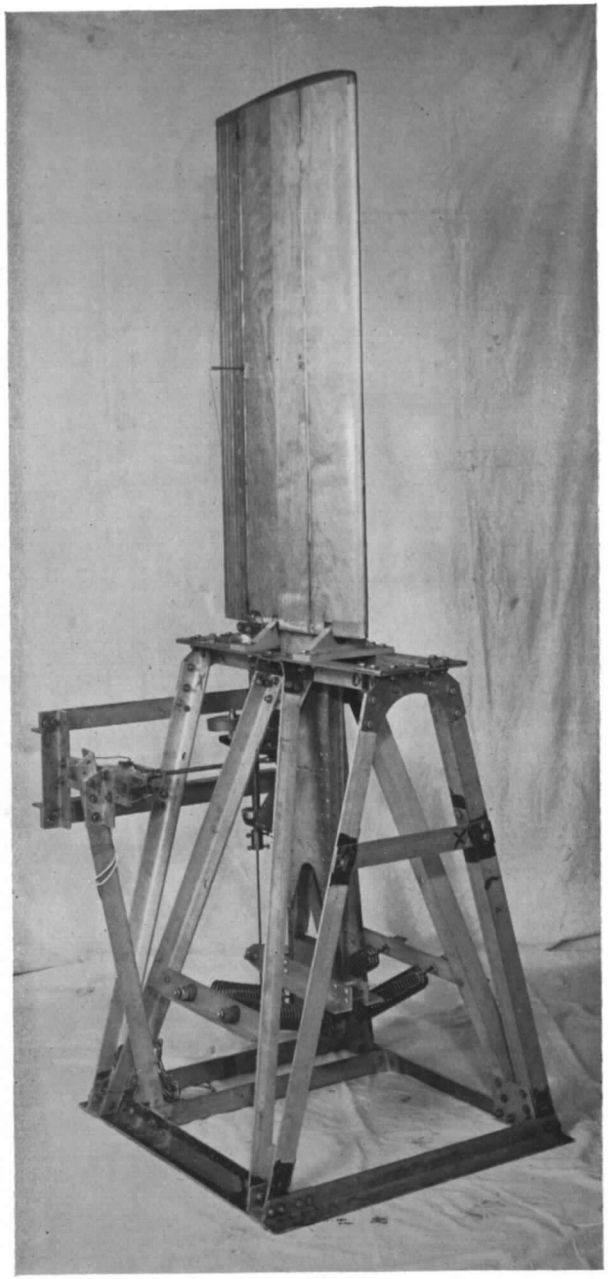

FIG. 2a. General view of rig.

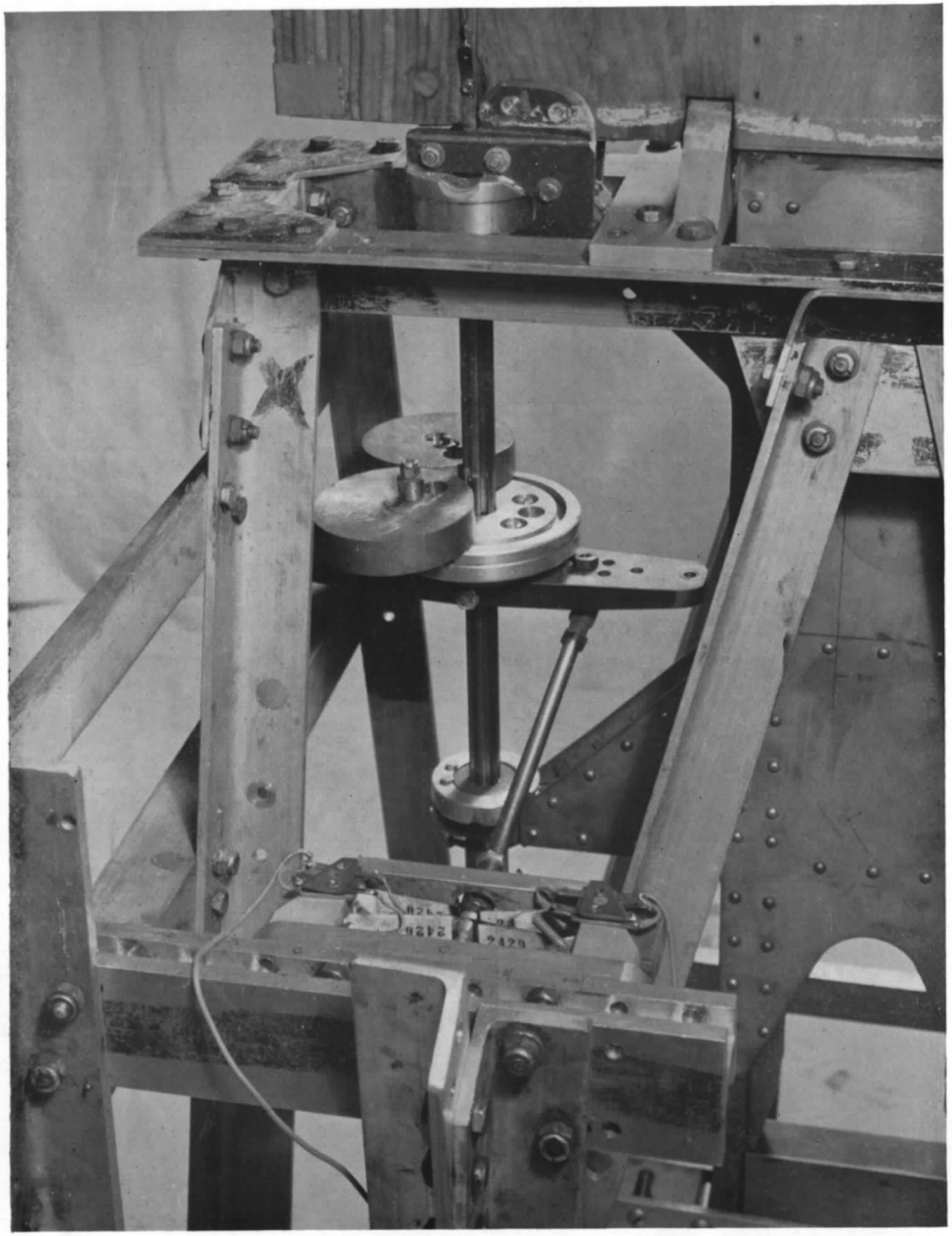

FIG. 2b. View of gearing system and inertia balance arrangement.

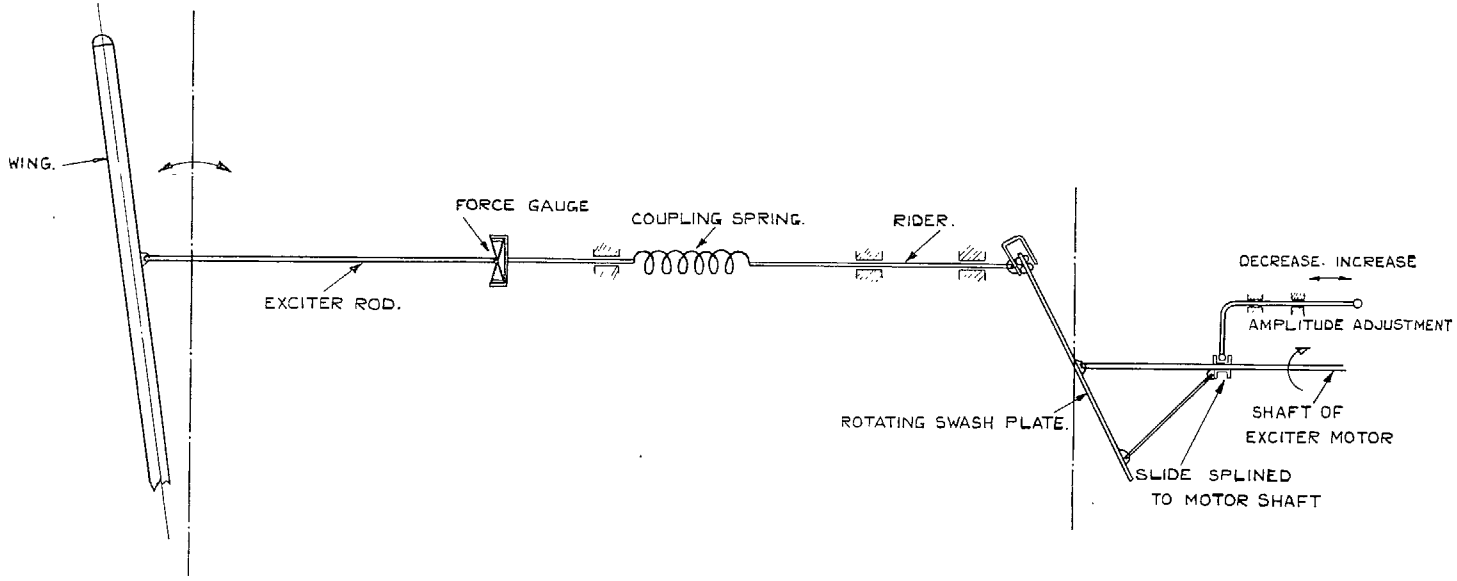

FIG. 3. Diagrammatic representation of excitation system.

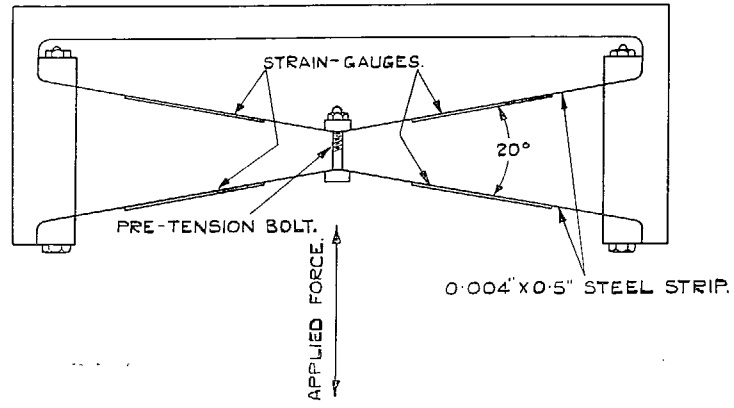

FIG. 4. Force-measuring gauge.

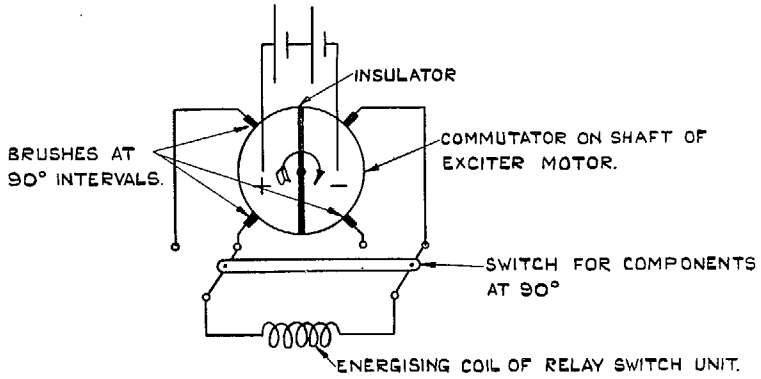

FIG. 5a. Square-wave generator. Force measurements.

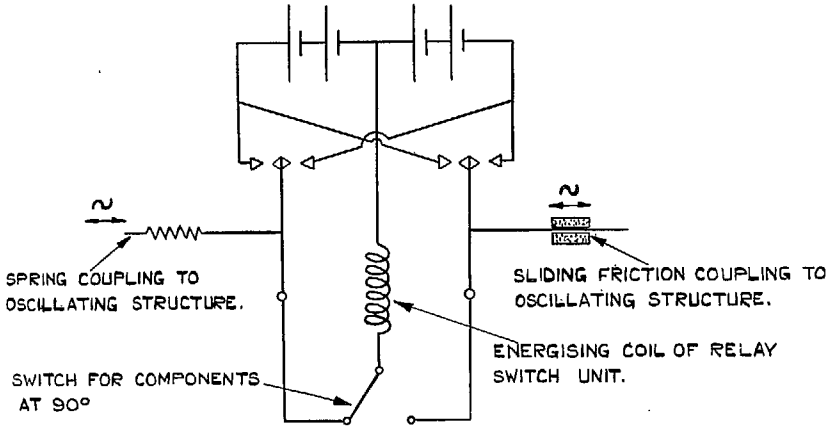

FIG. 5b. Square-wave generator. Flutter tests.

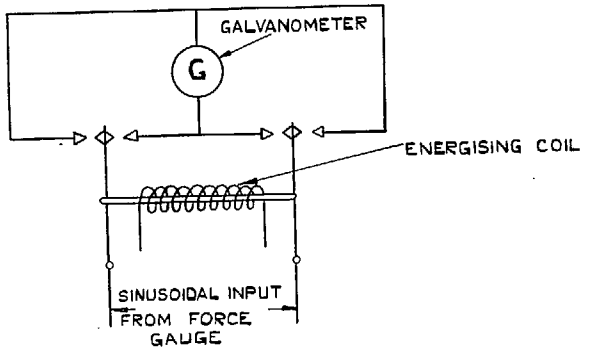

FIG. 5c. Relay switch unit.

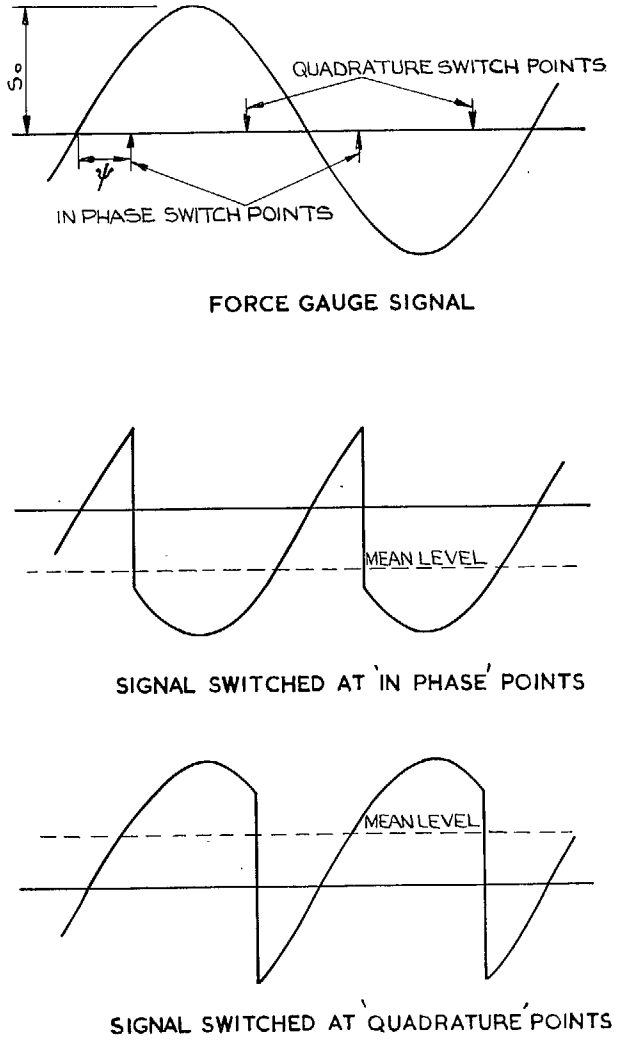

FIG. 6. Rectification by relay switch unit.

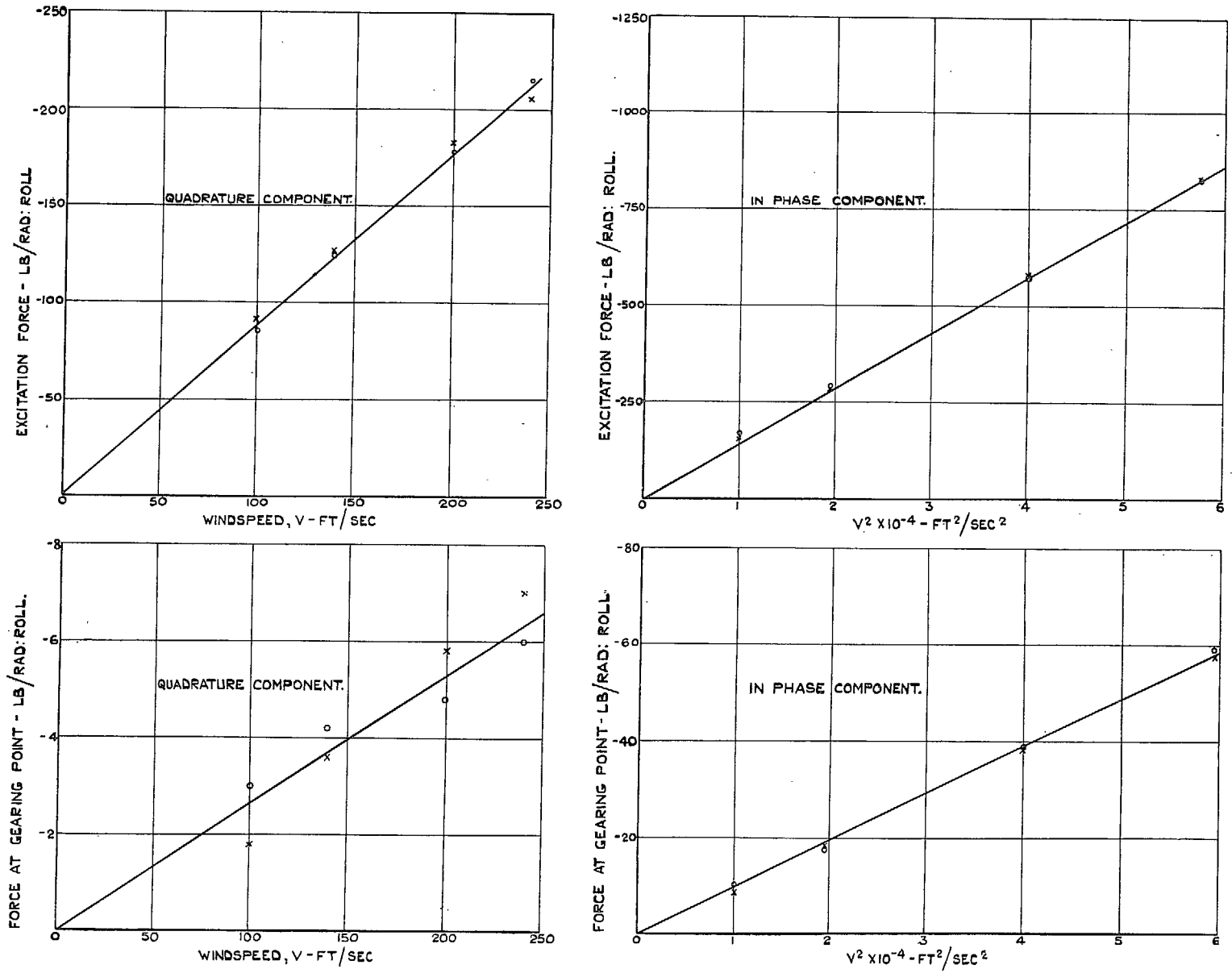

FIG. 7. Forces at excitation and gearing points : $\frac{\text{Aileron angle}}{\text{Roll angle}} = +2{\cdot}3$. Excitation frequency = 5·47 c.p.s.

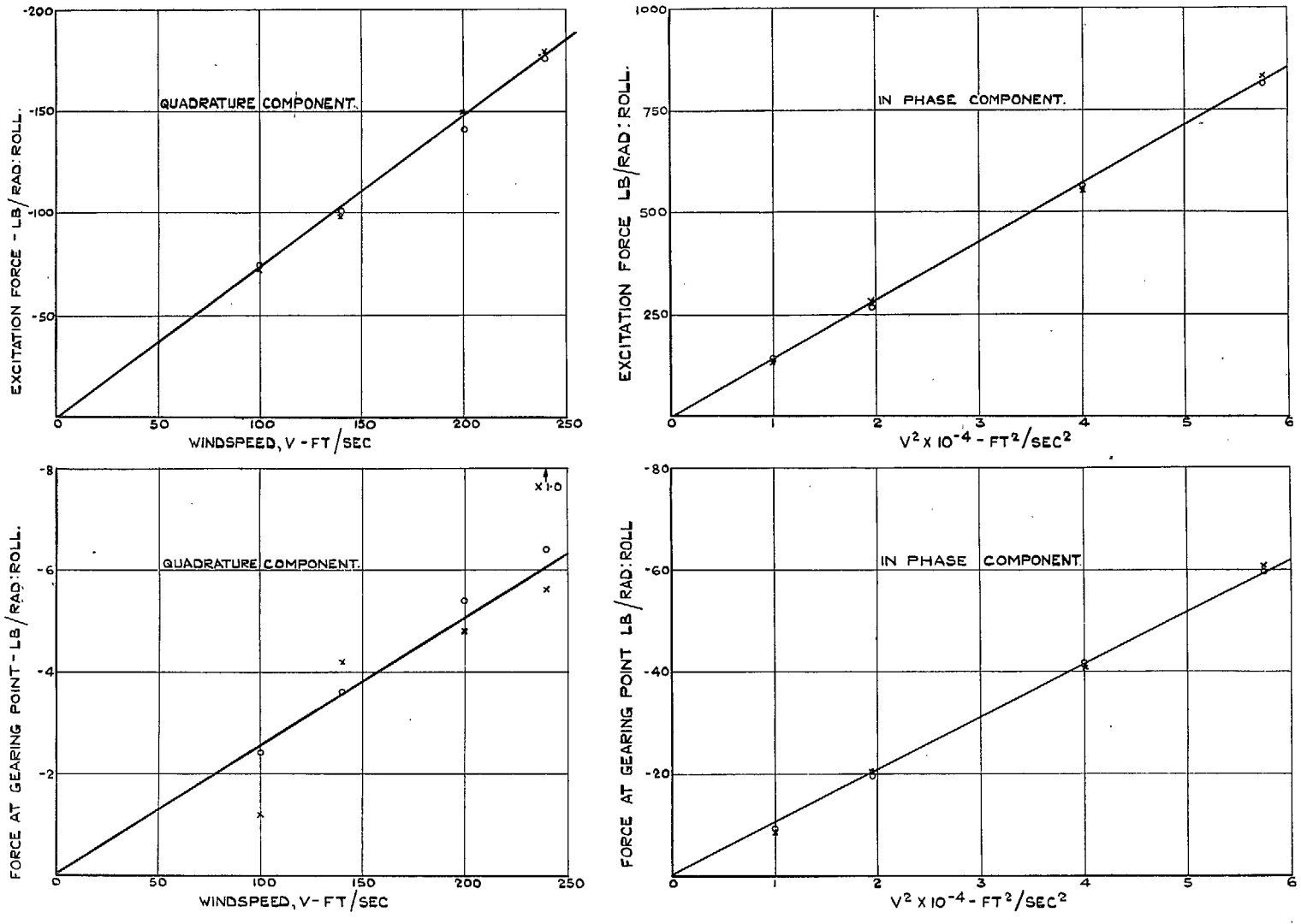

FIG. 8. Forces at excitation and gearing points : $\frac{\text{Aileron angle}}{\text{Roll angle}} = -2{\cdot}3$. Excitation frequency = 5·47 c.p.s.

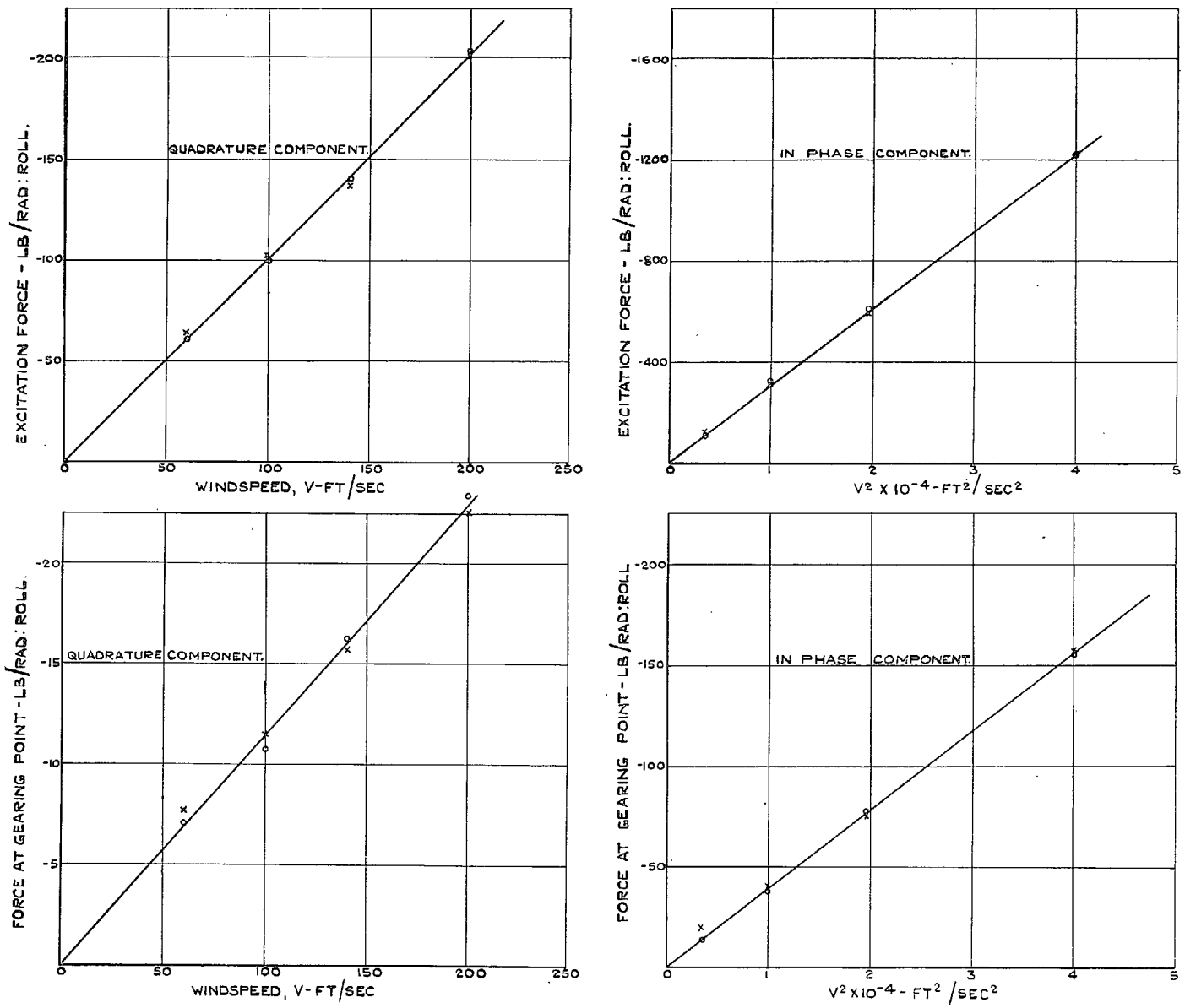

FIG. 9. Forces at excitation and gearing points: $\frac{\text{Aileron angle}}{\text{Roll angle}} = +4{\cdot}6$. Excitation frequency = 5·47 c.p.s.

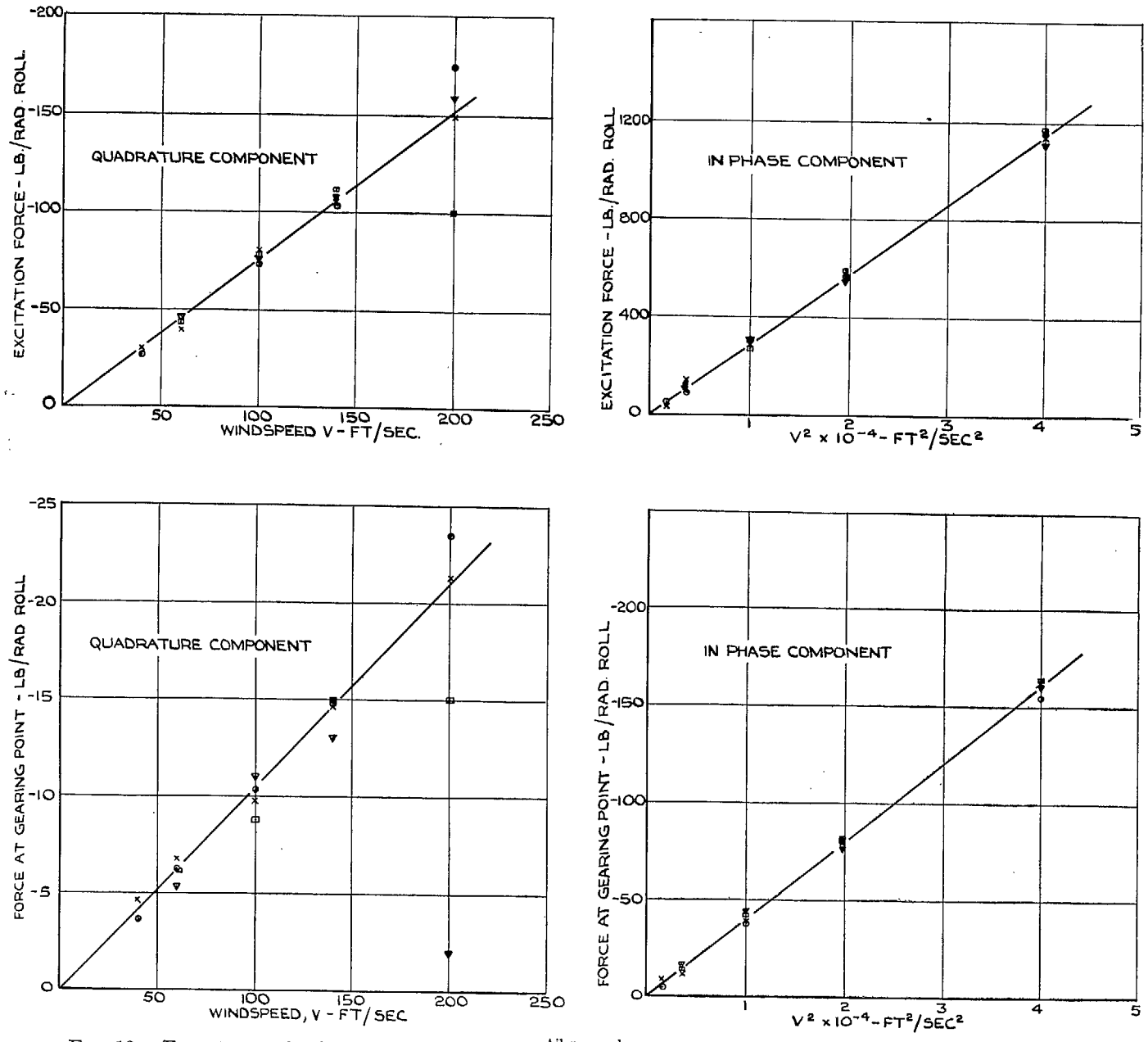

FIG. 10. Forces at excitation and gearing points : $\frac{\text{Aileron angle}}{\text{Roll angle}} = -4{\cdot}6$. Excitation frequency = 5·47 c.p.s.

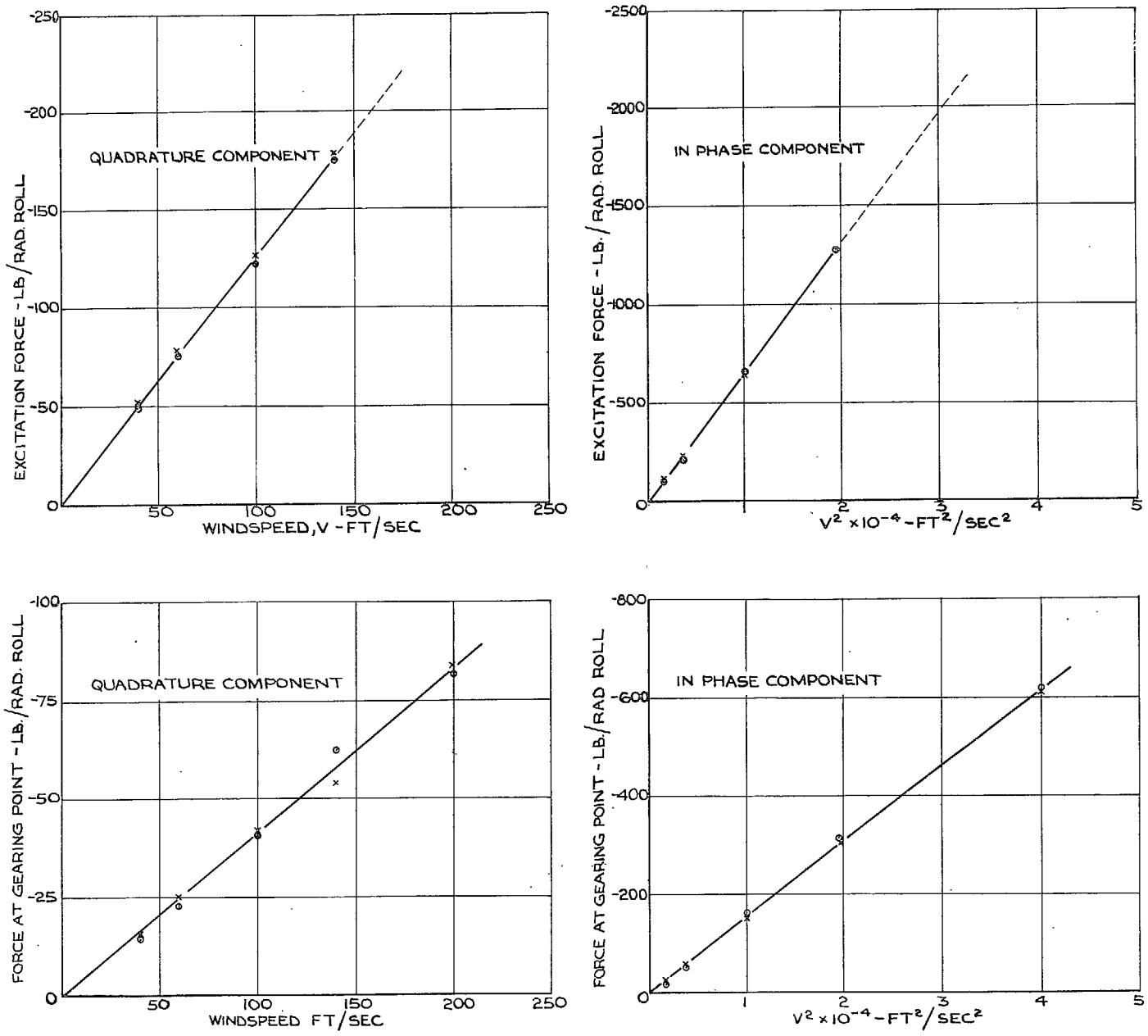

FIG. 11. Forces at excitation and gearing points : $\frac{\text{Aileron angle}}{\text{Roll angle}} = +9{\cdot}2$. Excitation frequency = 5·47 c.p.s.

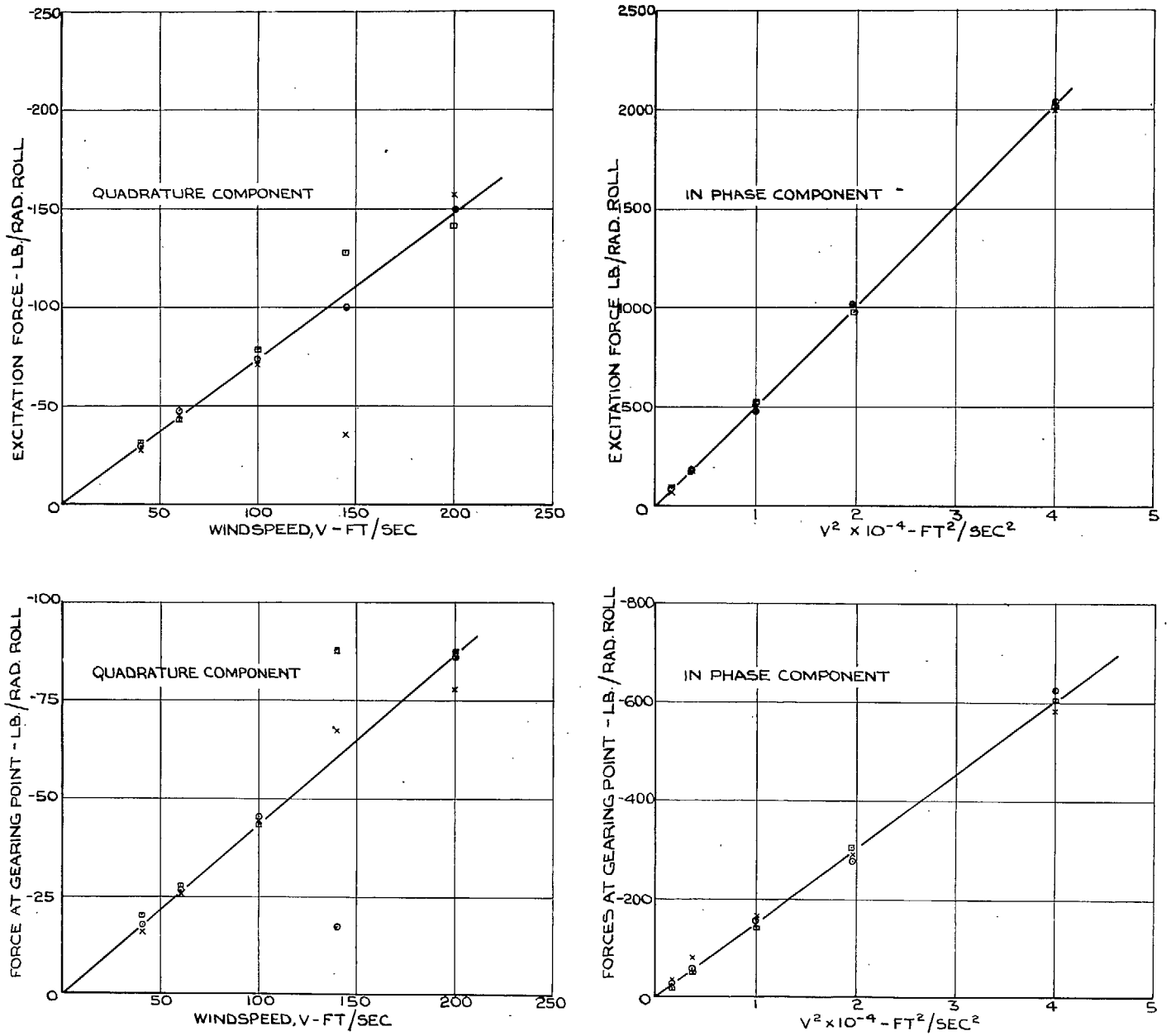

FIG. 12. Forces at excitation and gearing points : $\frac{\text{Aileron angle}}{\text{Roll angle}} = -9{\cdot}2$. Excitation frequency = 5·47 c.p.s.

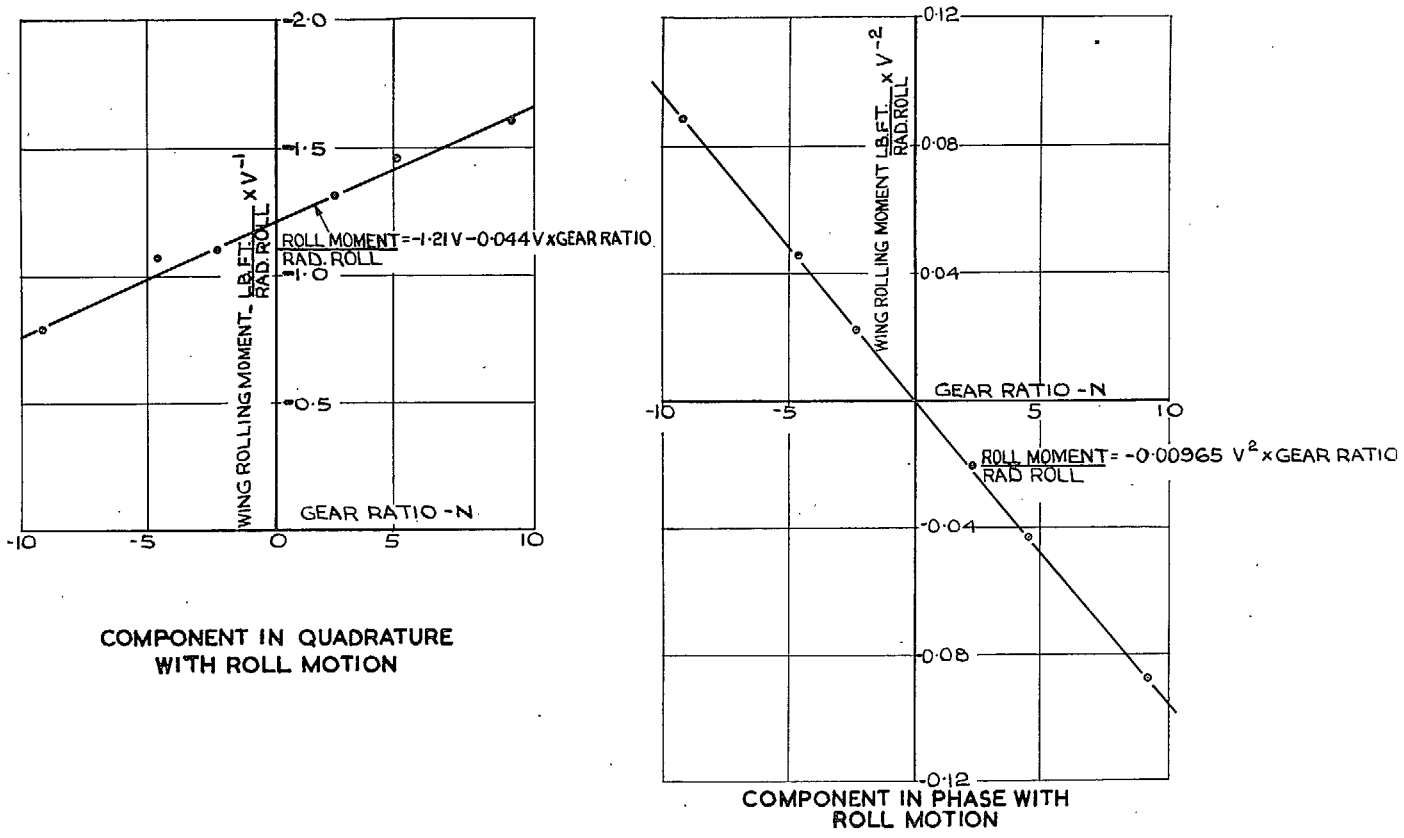

FIG. 13. Wing-rolling–moment functions plotted against gear ratio. Excitation frequency = 5·47 c.p.s.

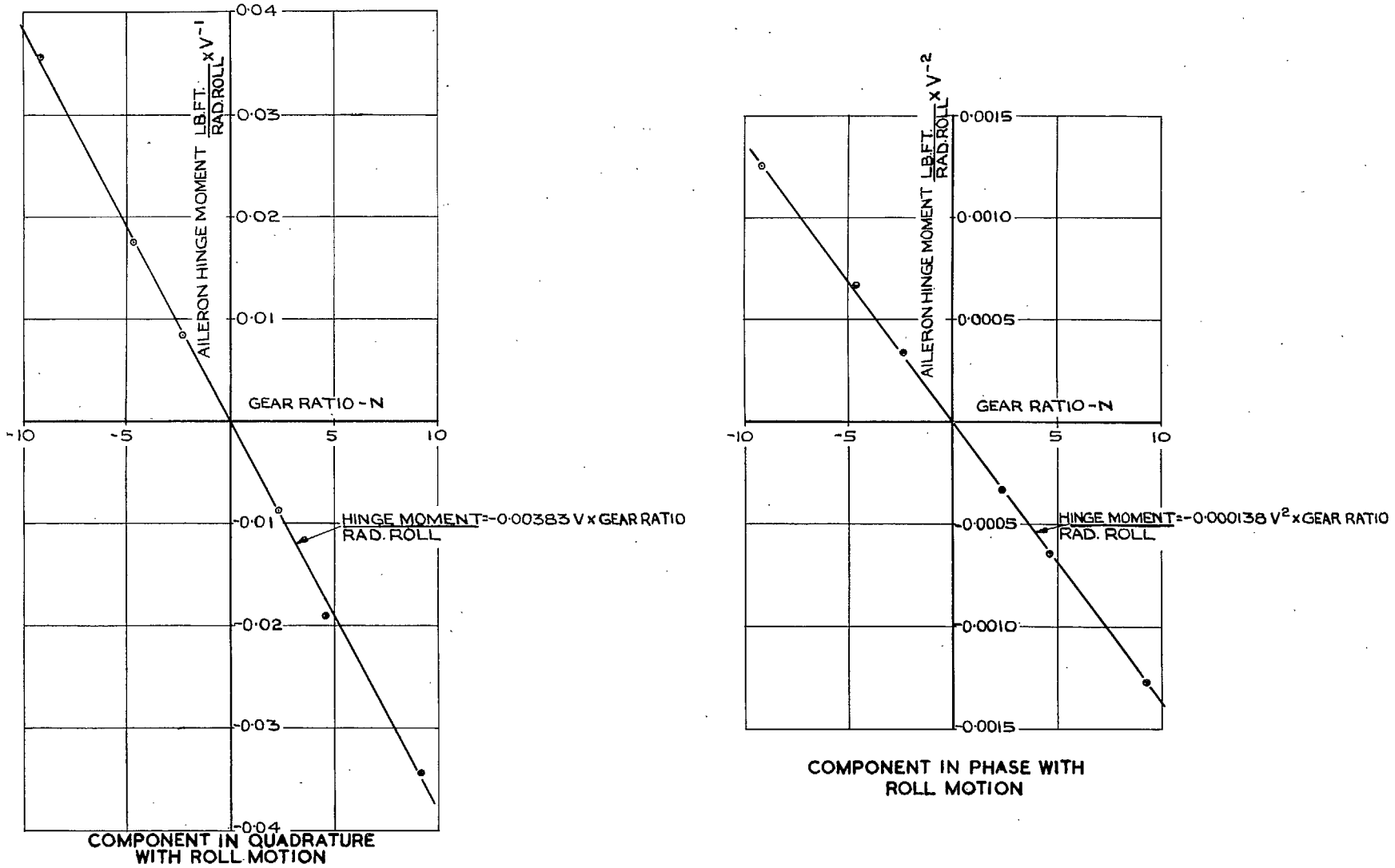

FIG. 14. Aileron-hinge–moment functions plotted against gear ratio. Excitation frequency = 5·47 c.p.s.

(5064) Wt. 20/9036 K.7 9/57 Hw.

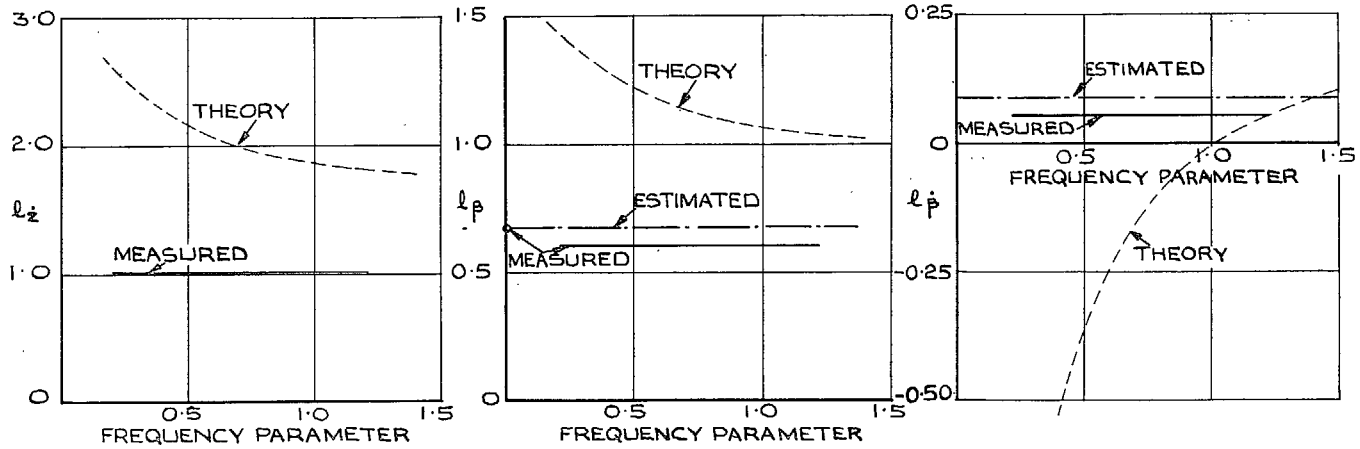

FIG. 15. Comparison of measured equivalent constant-strip derivatives with estimated derivatives and two-dimensional–theory values. Lift derivatives $l_{\dot{z}}$, l_β, $l_{\dot{\beta}}$.

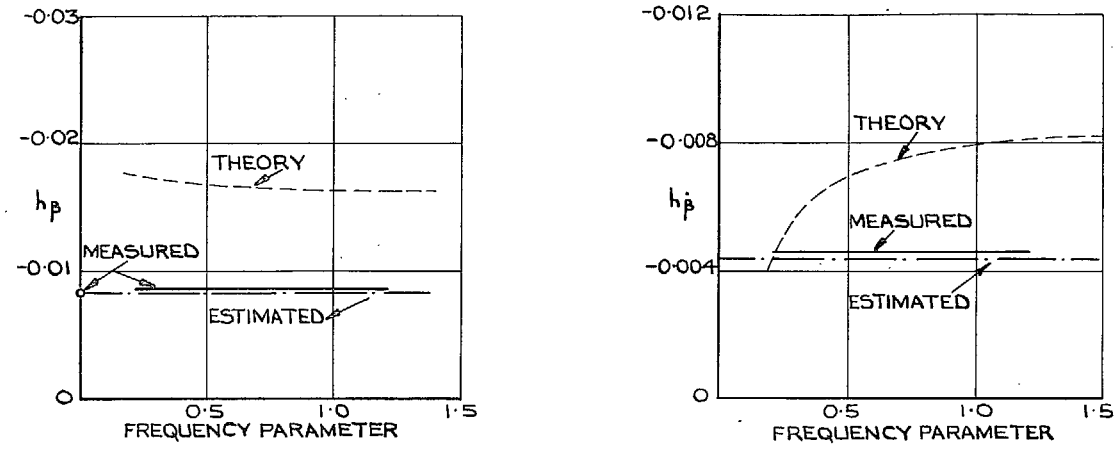

FIG. 16. Comparison of measured equivalent constant-strip derivatives with estimated derivatives and two-dimensional–theory values. Hinge-moment derivatives h_β, $h_{\dot{\beta}}$.

PRINTED IN GREAT BRITAIN

Publications of the Aeronautical Research Council

ANNUAL TECHNICAL REPORTS OF THE AERONAUTICAL RESEARCH COUNCIL (BOUND VOLUMES)

1939 Vol. I. Aerodynamics General, Performance, Airscrews, Engines. 50*s.* (51*s.* 9*d.*).
Vol. II. Stability and Control, Flutter and Vibration, Instruments, Structures, Seaplanes, etc. 63*s.* (64*s.* 9*d.*)

1940 Aero and Hydrodynamics, Aerofoils, Airscrews, Engines, Flutter, Icing, Stability and Control Structures, and a miscellaneous section. 50*s.* (51*s.* 9*d.*)

1941 Aero and Hydrodynamics, Aerofoils, Airscrews, Engines, Flutter, Stability and Control Structures. 63*s.* (64*s.* 9*d.*)

1942 Vol. I. Aero and Hydrodynamics, Aerofoils, Airscrews, Engines. 75*s.* (76*s.* 9*d.*)
Vol. II. Noise, Parachutes, Stability and Control, Structures, Vibration, Wind Tunnels. 47*s.* 6*d.* (49*s.* 3*d.*)

1943 Vol. I. Aerodynamics, Aerofoils, Airscrews. 80*s.* (81*s.* 9*d.*)
Vol. II. Engines, Flutter, Materials, Parachutes, Performance, Stability and Control, Structures. 90*s.* (92*s.* 6*d.*)

1944 Vol. I. Aero and Hydrodynamics, Aerofoils, Aircraft, Airscrews, Controls. 84*s.* (86*s.* 3*d.*)
Vol. II. Flutter and Vibration, Materials, Miscellaneous, Navigation, Parachutes, Performance, Plates and Panels, Stability, Structures, Test Equipment, Wind Tunnels. 84*s.* (86*s.* 3*d.*)

1945 Vol. I. Aero and Hydrodynamics, Aerofoils. 130*s.* (132*s.* 6*d.*)
Vol. II. Aircraft, Airscrews, Controls. 130*s.* (132*s.* 6*d.*)
Vol. III. Flutter and Vibration, Instruments, Miscellaneous, Parachutes, Plates and Panels, Propulsion. 130*s.* (132*s.* 3*d.*)
Vol. IV. Stability, Structures, Wind Tunnels, Wind Tunnel Technique. 130*s.* (132*s.* 3*d.*)

Annual Reports of the Aeronautical Research Council—

1937 2*s.* (2*s.* 2*d.*) 1938 1*s.* 6*d.* (1*s.* 8*d.*) 1939–48 3*s.* (3*s.* 3*d.*)

Index to all Reports and Memoranda published in the Annual Technical Reports, and separately—

April, 1950 - - - - R. & M. 2600 2*s.* 6*d.* (2*s.* 8*d.*)

Author Index to all Reports and Memoranda of the Aeronautical Research Council—

1909—January, 1954 R. & M. No. 2570 15*s.* (15*s.* 6*d.*)

Indexes to the Technical Reports of the Aeronautical Research Council—

December 1, 1936—June 30, 1939	R. & M. No. 1850	1*s.* 3*d.* (1*s.* 5*d.*)
July 1, 1939—June 30, 1945	R. & M. No. 1950	1*s.* (1*s.* 2*d.*)
July 1, 1945—June 30, 1946	R. & M. No. 2050	1*s.* (1*s.* 2*d.*)
July 1, 1946—December 31, 1946	R. & M. No. 2150	1*s.* 3*d.* (1*s.* 5*d.*)
January 1, 1947—June 30, 1947	R. & M. No. 2250	1*s.* 3*d.* (1*s.* 5*d.*)

Published Reports and Memoranda of the Aeronautical Research Council—

Between Nos. 2251–2349	R. & M. No. 2350	1*s.* 9*d.* (1*s.* 11*d.*)
Between Nos. 2351–2449	R. & M. No. 2450	2*s.* (2*s.* 2*d.*)
Between Nos. 2451–2549	R. & M. No. 2550	2*s.* 6*d.* (2*s.* 8*d.*)
Between Nos. 2551–2649	R. & M. No. 2650	2*s.* 6*d.* (2*s.* 8*d.*)

Prices in brackets include postage

HER MAJESTY'S STATIONERY OFFICE

York House, Kingsway, London, W.C.2; 423 Oxford Street, London, W.1; 13a Castle Street, Edinburgh 2; 39 King Street, Manchester 2; 2 Edmund Street, Birmingham 3; 109 St. Mary Street, Cardiff; Tower Lane, Bristol, 1; 80 Chichester Street, Belfast, *or through any bookseller.*

S.O. Code No. 23-3010